# 2D Linear Elasticity Using an Efficient Mollified Collocation Method with Local P-Adaptivity

**Syahrir Ginanjar[1*], Lavi Rizki Zuhal[1], Eky Febrianto[1,2]**

[1]Faculty of Mechanical and Aerospace Engineering, Institut Teknologi Bandung, Jalan Ganesa 10, Bandung 40132, Indonesia
[2]Glasgow Computational Engineering Centre, University of Glasgow, Glasgow, UK
[*]Email: 23623005@mahasiswa.itb.ac.id

**Abstract.** Point collocation method becomes popular in engineering design and analysis in which offers a significant advantage by employing discretized strong form, instead of being averaged over the domain as is the case in weak form approach. Mollified basis functions offer several advantages such as ease of constructing, flexible degree and smoothness, also adaptability to arbitrary partitions, in which formed by convolving local polynomials within a cell with a smooth kernel called mollifier. Since mollified basis functions have high order and smoothness, it is possible for us to do local refinement like p-adaptivity, where the polynomial order is chosen to be higher at certain region, one of the examples is stress concentration in linear elasticity problem. The local p-adaptivity implementation yields a higher convergence rate, resulting in computational efficiency. Furthermore, the study of mollified collocation method using local p-adaptivity is conducted by evaluating convergence error in linear elasticity plate with hole problem.

**Keywords:** *local p-adaptivity, mollified basis functions, point collocation method, linear elasticity.*

## 1 Introduction

Collocation methods are often more computationally efficient compared to Finite Element Method (FEM) [1]. Point Collocation Method or also known as PCM has been extensively explored and applied, one of the research is about the concept of stabilized Lagrange interpolation within the PCM which providing enhanced stability and accuracy [2]. The next is about weak form collocation method, which extends method to handle weak formulations of Partial Differential Equations [3]. The former researcher applied this method to linear elasticity problems and incorporated adaptivity to improve efficiency and accuracy [4].

Since the PCM connects discretization quantity with continuous quantity, the needs of basis functions become clear and the mollified basis functions offer

Received ________, Revised _________, Accepted for publication __________

several advantages. Mollified basis functions are inherently smooth and well-suited for collocation-based approaches. Additionally, these basis functions are also suitable for any refinements such as p-refinement which enables us to assign different polynomial orders within domain cells, h-refinement which involves increasing the number of cells $(n_c)$ and increase the total number of basis functions $(n_B)$ [5]. Mollified basis functions are also capable of solving higher order PDE such as biharmonic problem [6]. Because of that, it is possible for us to do local refinement to any problem whose solutions have higher gradient in the certain region, such as welding where a small area of the part is subjected to very high temperatures [7], while the temperature in the rest of the parts remain low, and stress concentration around hole in plate with hole problem [8].

As discussed in the former research, the number of basis functions depend on the polynomial order [5]. Since the mollified basis functions have an ability to arbitrary set polynomial order and it affects the number of basis function, we can set different polynomial order in our simulation to decrease the computational times. However, a significant challenge lies in the evaluation of mollified basis functions, as it requires the intersection algorithms from computational geometry to obtain the area for being convolution domain as mollification conducted.

In this paper, we will solve linear elasticity problem using mollified collocation method with local p-adaptivity, the research is conducted to analyze the effect of p-refinement on the convergence of $L^2$-norm, and $H^1$-semi-norm errors. Moreover, we will also study the number of collocation points $(n_k)$ especially around hole in term of convergence errors.

## 2 Review of Mollified Basis Functions

### 2.1 Mollification of Piecewise Polynomials

Convolutional smoothing methods is widely developed in engineering practice such as high-order convolution integral with the smooth kernel [9] and smooth convolution-based distance functions which computes an implicit $C^2$ smooth approximation on triangle meshes [10]. Another developments using convolution integral is mollified basis functions [5].

The process of obtaining convolutional smoothing for a one-dimensional domain $\Omega \in \mathcal{R}^1$ involves partitioning it into a collection of $n_c$ non-overlapping sections called cells, denoted as $\{\Omega_i\}$. Each cell represents a distinct section of the domain, such that

$$\Omega = \bigcup_{i=1}^{n_c} \Omega_i \tag{1}$$

On each cell, $\Omega_i$ a local polynomial is defined,

$$f_i(x) = \begin{cases} \boldsymbol{p}_i(x) \cdot \boldsymbol{\alpha}_i & \text{if } x \in \Omega_i \\ 0 & \text{if } x \notin \Omega_i \end{cases} \tag{2}$$

The local polynomial order $q^p$ is represented by the vector $\boldsymbol{p}_i(x)$, with $\alpha_{ii}$ being the corresponding polynomial coefficients, the result of mollification is shown in Fig. 1. The summation of local polynomials defined across the entire domain $\Omega$ yields the following result

$$f_i(x) = \sum_i \boldsymbol{p}_i(x) \cdot \alpha_i \tag{3}$$

It is important to take note that the function will be discontinuous across the cell boundaries, denoted as $f(x) \in \mathcal{C}^{-1}$. To enhance the smoothness of $f(x)$, the convolution with mollifier $m(x)$ will address the problem, where the mollifier has the following set of properties

$$m(x) \geq 0\,, \qquad \forall x \in \Omega \tag{4}$$

$$\operatorname{supp} m(x) = \left(-\frac{h_m}{2}, \frac{h_m}{2}\right) \tag{5}$$

$$\int_\Omega m(x)\ dx = 1 \tag{6}$$

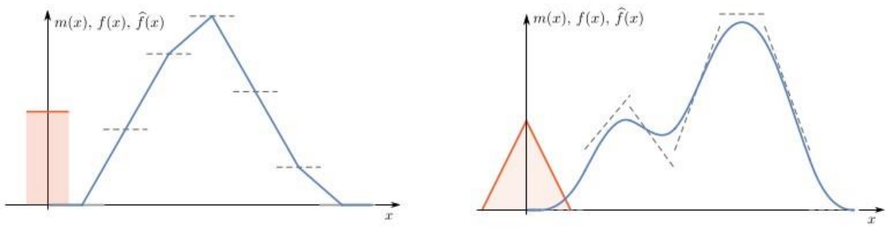


(A) (B)

**Figure 1** Mollification of piecewise discontinuous functions $f(x)$ (black, dashed) with a constant mollifier $m(x)$ (red, solid). The resulting mollified functions $\hat{f}(x)$ (blue, solid) are $\mathcal{C}^0$ continuous (A). Linear mollifier can be employed to obtain mollified functions with higher continuity $\mathcal{C}^1$ (B) [5]

The process of mollifying $f(x)$ involves defining it through convolution with the mollifier

$$\hat{f}(x) = m(x) * f(x) = \int_{\Omega} m(x-y) f(y)\, dy \tag{7}$$

Additionally, polynomial mollifiers $m(x)$ of degree $q^m$ are determined, while $f(x)$ is of degree $q^p$ as previously mentioned. It is evident that the maximum degree of the mollified function $\hat{f}(x)$ can be observed as $q^m + q^p + 1$. In the case where the derivative of the mollifier $m(x)$ exists, the derivative of mollified function $\hat{f}(x)$ can also be determined as

$$\frac{d}{dx}\hat{f}(x) = \int_{\Omega} \frac{dm(x-y)}{dx} f(y)\, dy \tag{8}$$

## 2.2 Basis Functions Construction

The mollification method is utilized to derive the basis functions for both single and multi-dimensional domains. The domain $\Omega \in \mathcal{R}^d$ is divided into a collection of non-overlapping convex polytopes $\{\Omega_i\}$ referred to as cells which then, for each cell, the mollification method generates a set of basis functions. Noting that, the support required for the mollified basis functions are determined by taking the Minkowski sum of the mollifier support with the corresponding cell [11].

### 2.2.1 Univariate Basis Function

Once the convolutional definition is derived, the process of deriving basis functions in the univariate case lies the foundation for extending it to the multivariate scenario. The basis functions specific to each cell, denoted as $\Omega_i$, can be expressed using the mollification as follows

$$f^m(x) = \sum_i \boldsymbol{\alpha}_i \boldsymbol{N}_i(x) \tag{9}$$

Where the mollified basis functions vector $\boldsymbol{N}_i(x)$ are defined by considering

$$\boldsymbol{N}_i(x) = \int_{\Omega_i} m(x-y) \boldsymbol{p}_i(y)\ dy \tag{10}$$

The selection of basis does not impact the approximation quality of the resulting mollified basis, it does affect the interpretability of the coefficient $\boldsymbol{\alpha}_i$ and the conditioning of the matrix [5]. Suppose that the monomial basis in each cell $\Omega_i$

$$\boldsymbol{p}_i(x) = \left(1\ \ x\, x^2 \ldots\, x^{q^p}\right) \text{ with } \ x = \frac{2(x-c_i)}{h} \tag{11}$$

Where $q^p$ represents the monomial degree, $c_i$ is center of cell, and $h$ denotes the average length of all cells $\{\Omega\}$ in the domain. The scaling factor of $\frac{2}{h}$ ensures that all mollified basis functions have a similar maximum value.

To evaluate the mollified basis function $\boldsymbol{N}_i(x)$ at a given point $x \in \Omega$ within the domain, we use convolution integral as shown in Eq. 13**.** In each case, the support size of the mollified basis functions is $h_m + h_{c,i}$, where $h_m$ denotes mollifier size and $h_{c,i} = x_{i+1} - x_i$ denotes the cell size.

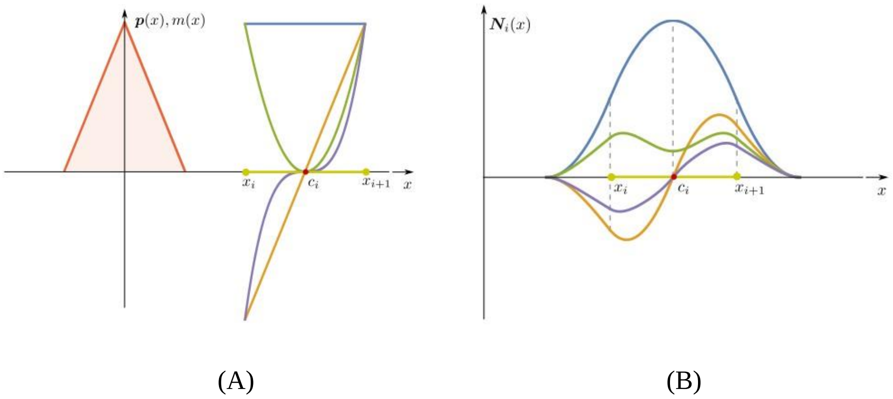


**Figure 2** Univariate mollified basis functions are examined in relation to bilinear mollifier ($q^m = 1$) and a cubic local polynomial ($q^p = 3$) within cell domain $\Omega_i = (x_{i+1}, x_i)$. The mollified basis functions shown in (B) are derived using mollifier as depicted in (A)

### 2.2.2 Multivariate Basis Function

Similar to univariate case, the basis functions associated with a cell $\Omega_i$ are defined as follows

$$\boldsymbol{N}_i(\boldsymbol{x}) = \int_{\Omega_i} m(\boldsymbol{x} - \boldsymbol{y})\boldsymbol{p}_i(\boldsymbol{y})\ dy \tag{12}$$

The vector $\boldsymbol{p}_i(x)$ consists of the multivariate monomial basis functions of degree $q^p$ which can be obtained by performing tensor product from univariate case, such that

$$m(\boldsymbol{x}) = m\left(x^{(1)}\right) \cdot m\left(x^{(2)}\right) \cdot m\left(x^{(3)}\right) \tag{13}$$

The mollifier can be constructed by $C^2$-continuous hexic splines

$$m(x) = \begin{cases} \frac{35}{16h_m}\left(1 - 12\left(\frac{x}{h_m}\right)^2 + 48\left(\frac{x}{h_m}\right)^4 - 64\left(\frac{x}{h_m}\right)^6\right) & \text{if } |x| < \frac{h_m}{2} \\ 0 & \text{if } |x| \geq \frac{h_m}{2} \end{cases} \tag{14}$$

Where it has 6 boundary conditions such that $m\left(-\frac{h_m}{2}\right) = m\left(\frac{h_m}{2}\right) = 0$, $\frac{dm}{dx}\left(-\frac{h_m}{2}\right) = \frac{dm}{dx}\left(\frac{h_m}{2}\right) = 0$ and $\frac{d^2m}{dx^2}\left(-\frac{h_m}{2}\right) = \frac{d^2m}{dx^2}\left(\frac{h_m}{2}\right) = 0$ The continuity of the mollifier can be further enhanced by imposing additional zero derivatives at $x = -\frac{h_m}{2}$ and $x = \frac{h_m}{2}$. However, both approaches increase computational cost associated with convolution integrals evaluation.

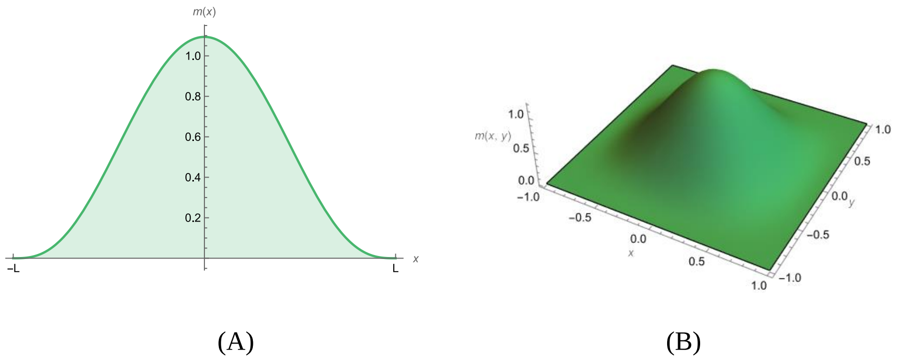


**Figure 3** $C^2$-continuous hexic splines mollifier with the mollifier width $h_m = 2$ for (A) univariate and (B) multivariate case.

## 3 Collocation Method

In this section, we will outline the discretization procedure within the collocation method for solving linear elasticity problems. This approach will then be applied to a plate with circular hole problem, where stress concentration effects are observed around the hole [7].

## 3.1 Discretization on Elasticity Problems

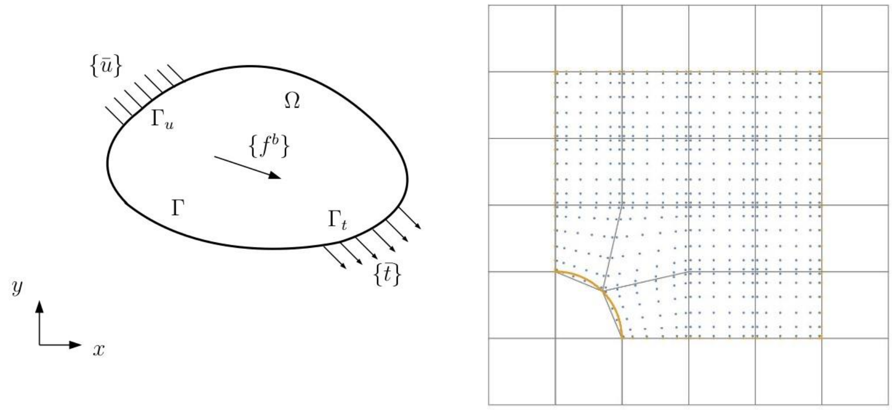


(A) (B)

**Figure 4** 2D problem domain subjected to the body force and boundary conditions (A) and (B) cell visualization with $h_c = \frac{1}{4}$

Based on Fig. 8, we know that the boundary $\Gamma = (\Gamma_u \cup \Gamma_t)$. The domain is subjected to external tractions $\{t\} = \{\overline{t_x}, \overline{t_y}\}^T$ applied on the Neumann boundary $\Gamma_t$, and prescibed displacements $\{\bar{u}\} = \{\overline{u_x}, \overline{u_y}\}^T$ on the Dirichlet boundary $\Gamma_u$. The vector $\{f^b\} = \{f_x^b, f_y^b\}^T$ represent the body force per unit volume. The governing equations and two distinct bouondary conditions are expressed below

$$[L]\{\sigma\} = \{f^b\} \quad \text{in } \Omega \tag{15}$$

$$\{u\} = \{\bar{u}\} \quad \text{on } \Gamma_u \tag{16}$$

$$[n]^T\{\sigma\} = \{\bar{t}\} \quad \text{on } \Gamma_t \tag{17}$$

Where $[L]$ is a differential operators matrix as follows

$$[L] = \begin{bmatrix} \frac{\partial}{\partial x} & 0 \\ 0 & \frac{\partial}{\partial y} \\ \frac{\partial}{\partial y} & \frac{\partial}{\partial x} \end{bmatrix} \tag{18}$$

The vector of Cauchy stress $\{\sigma\}$ in 2D is given as

$$\{\sigma\} = \{\sigma_{xx}, \sigma_{yy}, \sigma_{xy}\}^T \tag{19}$$

Which means $\sigma_{xx}$ and $\sigma_{yy}$ are normal stress and $\sigma_{xy}$ is shear stress. The vector of $\{u\}$ is the field variable represented as

$$\{u\} = \{u_x, u_y\}^T \tag{20}$$

And $[N]$ is an outer normals matrix of a point residing on the boundary, which expressed as

$$[N] = \begin{bmatrix} n_x & 0 \\ 0 & n_y \\ n_y & n_x \end{bmatrix} \tag{21}$$

The connection between stress and strain in this material is

$$\{\sigma\} = [D]\{\epsilon\} \tag{22}$$

For plane strain, the stiffness matrix $[D]$ of material is given by

$$[D] = \frac{E}{(1+\nu)(1-2\nu)} \begin{bmatrix} 1-\nu & \nu & 0 \\ \nu & 1-\nu & 0 \\ 0 & 0 & \frac{1-2\nu}{2} \end{bmatrix} \tag{23}$$

Hence, we obtain the governing equations and boundary conditions as follows

$$[L]^T[D]([L]\{u\}) = \{f^b\} \quad \text{in } \Omega \tag{24}$$

$$\{u\} = \{\bar{u}\} \quad \text{on } \Gamma_u \tag{25}$$

$$[n]^T[D]([L]\{u\}) = \{\bar{t}\} \quad \text{on } \Gamma_t \tag{26}$$

Considering that we deal with multi degrees of freedom, applying Lagrange multipliers is a common technique used to enforce constraints on the system. [12]

## 3.2 Local P-Adaptivity

Local p-adaptivity or also known as local p-refinement is one of method in Finite Element Analysis (FEA) that is applied by increasing the polynomial order in certain regions where higher accuracy is required such as areas with steep gradients, stress concentrations [8], high temperature [7]. Local p-adaptivity is widely used because of its capability of increasing efficiency in computational resources, higher accuracy with fewer elements and better handling of singularities or stress concentrations [13].

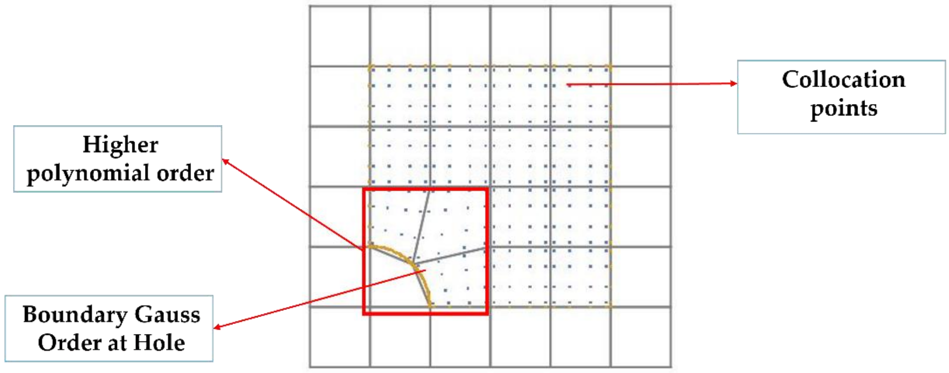


**Figure 5** Local p-adaptivity implementation on plate with hole simulation using mollified collocation method

# 4 Numerical Examples

## 4.1 One Dimensional Example

We consider the solution of the one-dimensional Poisson-Dirichlet problem

$$-\frac{d^2u(x)}{dx^2} = f(x) \tag{27}$$

On the domain $\Omega = (0,1) \in \mathcal{R}^1$. The source term $f(x)$ is chosen such that the soultion is equal to $u(x) = e^{-16x}$. As $f(x)$ is a decay function which means it has the higher gradient in the certain region relatives to the surroundings, we can apply local p-adaptivity in the region with higher gradient. First, construct the mollified basis functions, we define the non-overlapping cells $\{\omega_i\}_{i=1}^{n_c}$ of size $h_{c,i}$ where we define the piecewise polynomial basis functions $\boldsymbol{p}_i(x)$. We then consider the uniform cells $h_c \in \left\{\frac{1}{5}, \frac{1}{10}, \frac{1}{20}, \frac{1}{40}\right\}$ with $n_c \in \{7,12,22,42\}$ and the local polynomial $r_p \in \{1,2,3\}$, the mollifier width $(h_m)$ is set to be twice of the maximum cell size in one simulation.

We next distribute collocation points using Gauss quadrature points, which are distributed by mapping the standard Gauss quadrature from the parametric domain onto each cell [6]. For uniform refinement, we increase the number of cell and minimize the cell size .

After conducting uniform refinement simulation, we then consider the region that is having higher gradient, we choose that $\Omega_{refined} = [0,0.4]$. The p-refinement will consider the combination of quadratic-linear, cubic-linear, and cubic-quadratic.

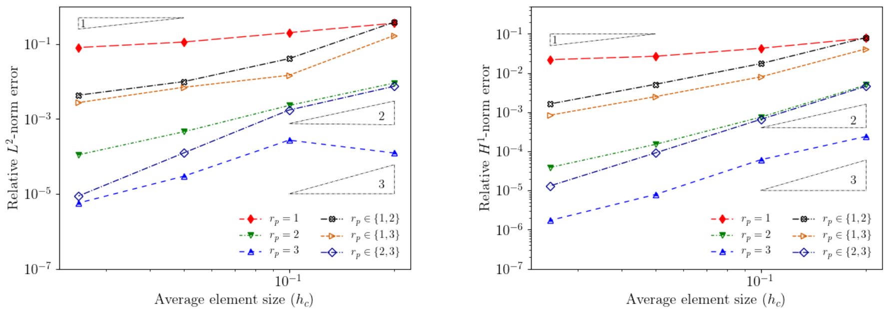


(A) (B)

**Figure 6** $L^2$-norm error (Left) and $H^1$-semi-norm error of 1D Poisson with decay function as the solution

The Fig. 5 shows a comparison of relative $L^2$-norm and $H^1$-semi-norm as a function of the average element size ($h_c$). The convergence behavior is analyzed for different refinement strategies, specifically local p-adaptivity and uniform refinement, with the goal of having lower error and computational efficiency. It shows that the higher of $r_p$ will lead to lower error and faster convergence by considering the convergence rate, it also can be seen with the local p-adaptivity error curves. Furthermore, $H^1$-seminorm is smoother than $L^2$-norm because of the smoothness characteristic of mollification, considering that $H^1$-seminorm is sensitive to error in gradient.

## 4.2 Plate With Hole

The classic linear elasticity problem is an infinite plate with a circular hole subjected to $\sigma = 10^6\ MPa$ far-field traction in the $x$-direction.

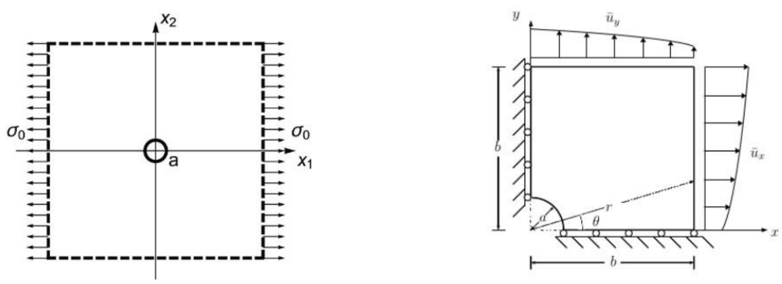


(A) (B)

**Figure 7** Infinite plate with hole with uniaxial loading case (A) and Model simulation of linear elasticity of plate with hole (B) [8]

The infinite plate with hole problem has been widely used for validation in the past and has an analytical displacement solution [7] which can be expressed as

$$u_x = \frac{Fa}{8\mu}\left[\frac{r}{a}(\kappa+1)\cos(\theta) + \frac{2a}{r}\big((1+\kappa)\cos(\theta)+\cos(3\theta)\big) - \frac{2a^3}{r^3}\cos(3\theta)\right] \tag{28}$$

$$u_x = \frac{Fa}{8\mu}\left[\frac{r}{a}(\kappa+1)\cos(\theta) + \frac{2a}{r}\big((1+\kappa)\cos(\theta)+\cos(3\theta)\big) - \frac{2a^3}{r^3}\cos(3\theta)\right] \tag{29}$$

The material properties utilized include a Young's modulus $E$ of 70 Gpa and Poisson's ratio $\nu$ of 0.3.

### 4.2.1 Displacement Visualization

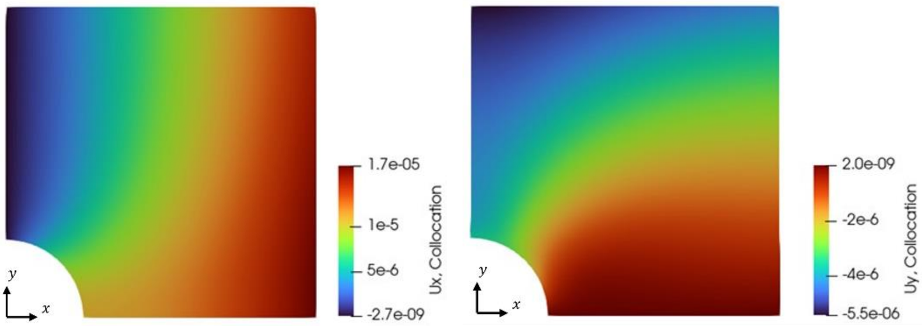


(A) (B)

**Figure 8** Visual comparison results of $x$ displacement (A) and $y$ displacement (B) between analytical and Mollified Collocation Method of linear elasticity problem in plate with hole

Since, the bottom and left of plate, the boundary conditions applied to the plate is roller, so that it can counters the displacement comes from stress applied. The plate will have larger displacement in $y$-direction at the bottom and larger displacement at $x$-direction at location far from hole

### 4.2.2 Stress Visualization

As mentioned in Eq. 24 that we will have 2 kinds of stresses, there are normal stress and shear stress. Normal stress is occurred at normal $x$ and normal $y$ direction where shear stress is occurred at plane $xy$.

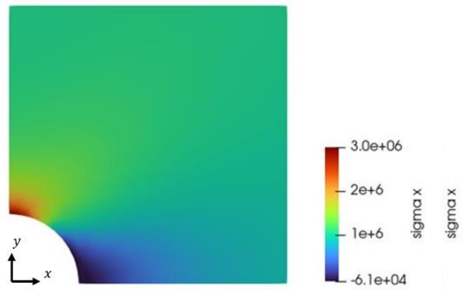


(A)

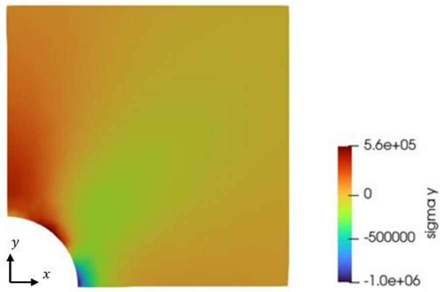


(B)

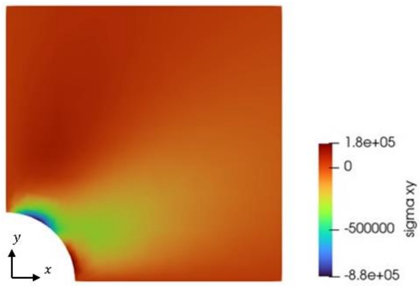


(C)

**Figure 9** Visual comparison of normal stress in $x$-direction (A), normal stress in $y$-direction (B), and shear stress at $xy$-plane (C) of 2D Linear Elasticity plate with hole problem.

As we can see from Fig. 9 that the normal stress around the circular hole is quite larger than the area far from the hole. It means that there is stress concentration around the circular hole. Also, from shear stress visualization we can see that the top side of circular hole will have lower shear stress than surroundings area.

## 4.3 The Convergence Error

We will analyze the convergence error by computing $L^2$-norm and $H^1$-semi-norm. We will analyze the effect of local p-adaptivity to the convergence error, and the number of collocation points around the circular hole to the convergence error.

### 4.3.1 The Effect of Local P-Adaptivity on Convergence Error

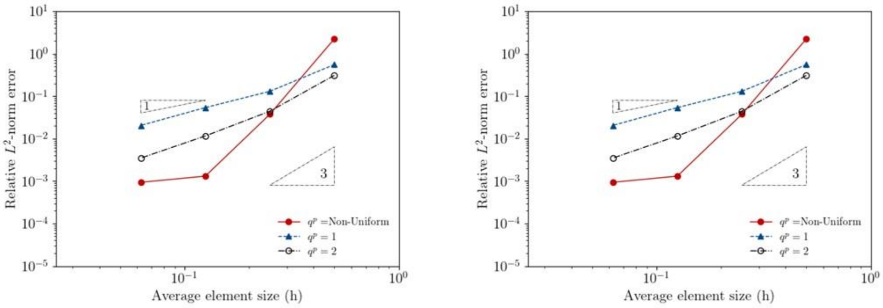


(A) (B)

**Figure 10** $L^2$-norm (A) and $H^1$-semi-norm (B) error for linear (blue, dot), quadratic (black, dashed) and p-adaptivity strategy (red) on plate with hole simulation

As we can see from Fig. 10, the higher local polynomial degree we use, we will have higher convergence rate. Also, by applying the local p-adaptivity, we will have lower error than the others.

### 4.3.2 The Effect of Boundary Collocation Points at Circular Hole

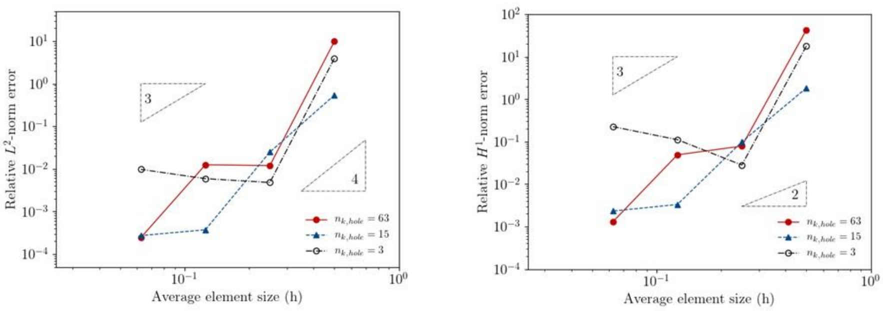


(A) (B)

**Figure 11** $L^2$-norm (A) and $H^1$-semi-norm error (B) for $n_{k@hole} = 3$ (black, dashed) $n_{k@hole} = 15$ (blue, dot), and $n_{k@hole} = 63$ (red) on plate with hole simulation

As shown in Fig. 11, the number of collocation points around the circular hole (denoted as $n_{k@hole}$) influences the convergence error. However, increasing the number of collocation points does not necessarily lead to improved accuracy. This is because the number of collocation points also affects the condition number of the Left-Hand Side (LHS) matrix, which can impact the stability of the numerical solution. Moreover, due to the discrete nature of the cells, the circular hole is not perfectly circular, introducing a stochastic error into the model.

## 5 Conclusion

The mollified basis functions can be effectively applied to the point collocation method for solving linear elasticity problems. Additionally, we can employ local p-adaptivity by increasing the local polynomial order in specific regions of the cell domain, such as near the hole in this case. This approach demonstrates that local p-adaptivity results in lower errors compared to using a uniform polynomial order throughout the domain. Moreover, local p-adaptivity provides a higher convergence rate, compared to solely using one order of local polynomial approach. It also provides more efficiency because it needs lower total number of basis functions than the uniform refinement.

Furthermore, the placement of boundary collocation points significantly influences the convergence error. Since these points are distributed across the cells and the circular hole is not perfectly circular due to cell shapes, the evaluation of the mollified basis functions becomes crucial. By evaluating the basis functions consistently at each point, the method ensures stability. However, the irregularity in the shape of circular hole introduces stochastic effects, which must be accounted for in the next research related to this topic.

## Acknowledgement

This work is as collaboration between the Flow Science and Engineering Lab in Faculty of Mechanical and Aerospace Engineering with University of Glasgow.

## References

[1] D. Schilinger, J. A. Evans, F. Frischmann, R. R. Hiemstra, M.-C. Hsu, and T. J. Hughes, "A collocated c0 finite element method: Reduced quadrature perspective, cost comparison with standard finite elements, and explicit structural dynamics," *International Journal for Numerical Methods in Engineering*, vol. 102, no. 3-4, pp. 576–631, 2015.

[2] L. Wang, M. Hu, Z. Zhong, and F. Yang, "Stabilized lagrange interpolation collocation method: A meshfree method incorporating the advantages of finite element method," *Computer Methods in Applied Mechanics and Engineering*, vol. 404, p. 115780, 2023.

[3] T. Oliveira and A. Portela, "Weak-form collocation – a local meshless method in linear elasticity," *Engineering Analysis with Boundary Elements*, vol. 73, pp. 144–160, 2016.

[4] L. Fan, W. M. Coombs, and C. E. Augarde, “The point collocation method with a local maximum entropy approach,” *Computers & Structures*, vol. 201, pp. 1–14, 2018.

[5] E. V. Febrianto, *Mollified piecewise polynomial approximants of arbitrary order and smoothness*. PhD thesis, University of Cambridge, 2019.

[6] D. Alfarisy, L. Zuhal, M. Ortiz, F. Cirak, and E. Febrianto, “Point collocation with mollified piecewise polynomial approximants for high-order partial differential equations,” *International Journal for Numerical Methods in Engineering*, Jun. 2024. [Online]. Available: http://dx.doi.org/10.1002/nme.7548

[7] D. Alves do Carmo and A. Rocha de Faria, “A 2d finite element with through the thickness parabolic temperature distribution for heat transfer simulations including welding,” *Finite Elements in Analysis and Design*, vol. 93, pp. 85–95, 2015. [Online]. Available: https://www.sciencedirect.com/science/article/pii/S0168874X14001851

[8] S. Timoshenko and J. N. Goodier, Theory of Elasticity. New York: McGraw-Hill, 1970.

[9] J. Qiang, “A high-order fast method for computing convolution integral with smooth kernel,” *Computer Physics Communications*, vol. 181, no. 2, pp. 313–316, 2010.

[10] A. Schmeißer, R. Wegener, D. Hietel, and H. Hagen, “Smooth convolution-based distance functions,” *Graphical Models*, vol. 82, pp. 67–76, 2015.

[11] F. Aurenhammer, “Voronoi diagrams—a survey of a fundamental geometric data structure,” ACM *Computing* Surveys, vol. 23, pp. 345–405, 1991.

[12] C. Felippa, *Introduction to Finite Element Methods*. Department of Aerospace Engineering Sciences and Center for Aerospace Structures University of Colorado, 2003.

[13] Demkowicz, L. (2006). Computing with hp-ADAPTIVE FINITE ELEMENTS: Volume 1 One and Two Dimensional Elliptic and Maxwell Problems (1st ed.). Chapman and Hall/CRC. https://doi.org/10.1201/9781420011685